

Analysis of ferroresonance in a neutral grounding system with nonlinear core loss

Hui Meng(惠 萌), Zhang Yan-Bin(张彦斌), and Liu Chong-Xin(刘崇新)

School of Electrical Engineering, Xi'an Jiao Tong University, Xi'an 710049, China

(Received 7 November 2008; revised manuscript received 18 November 2008)

The chaotic behaviour exhibited by a typical ferroresonant circuit in a neutral grounding system is investigated in this paper. In most earlier ferroresonance studies the core loss of the power transformer was neglected or represented by a linear resistance. However, this is not always true. In this paper the core loss of the power transformer is modelled by a third order series in voltage and the magnetization characteristics of the transformer are modelled by an 11th order two-term polynomial. Extensive simulations are carried out to analyse the effect of nonlinear core loss on transformer ferroresonance. A detailed analysis of simulation results demonstrates that, with the nonlinear core loss model used, the onset of chaos appears at a larger source voltage and the transient duration is shorter.

Keywords: ferroresonance, chaotic behaviour, nonlinear core loss

PACC: 0545, 0547

1. Introduction

Ferroresonance is a nonlinear phenomenon that often happens in power systems. In recent years the number of ferroresonance accidents has increased due to network complexity and the constant upgrading of equipment efficiency.^[1,2] Therefore, this nonlinear phenomenon in RCL circuits^[3–5] and power systems has been intensively investigated.^[6–11]

Ferroresonance is a complicated nonlinear phenomenon, which is caused by magnetic saturation. It originates from improper switching operation, routine switching, or load shedding involving a high voltage transmission line.^[12] It could generate unpredictable overvoltage and overcurrent. This may be harmful to power systems. In addition, which kind of transformer model is used is an important problem in ferroresonance study. This problem has received much attention. In Ref.[4] ferroresonance in an RCL series electric circuit was investigated in order to strengthen the effect of the magnetization phenomenon in the ferromagnetic core. In Ref.[5], the effect of different magnetization curves on the ferroresonance was discussed. In Refs.[6–12] the chaotic behaviour of ferroresonance in a power system was analysed. However, in Refs.[6–11] the core loss of the transformer was taken as a linear resistance. In order to increase the accuracy in ferroresonance study, a dynamic core loss is adopted in Refs.[12, 13], which makes the results more accu-

rate. Investigated in the present paper is the general chaotic behaviour of a typical ferroresonant circuit in a neutral grounding system with nonlinear core loss.

2. System modelling

In neutral grounding systems, a typical configuration of a substation prone to ferroresonance is shown in Fig.1,^[7] where D0 is the coupling breaker of the bus, D1 and D2 are circuit breakers, Ds is the disconnect switch, PT1 and PT2 are the potential transformers (PTs) connected to the bus, and VT1 and VT2 are the voltage transformers (VTs). When the ferroresonance is at onset, because the connectors and disconnect switches are all open, the voltage transformers are not in the ferroresonant circuit. Figure 2 is a Thevenin equivalent circuit of Fig.1. In this study, the PT is modelled as a nonlinear flux-controlled inductance L_2 , and the nonlinear resistance R_2 represents core loss of PT. Furthermore, R_1 and L_1 represent the resistance and leakage inductance of primary winding. C is a Thevenin equivalent capacitance of grading capacitance of the circuit breaker and phase to ground capacitance. For very high currents the ferromagnetic core might be driven into saturation where the flux-current characteristic is modelled as a polynomial^[5]

$$i_L = a\varphi + b\varphi^n, \quad (1)$$

[†]Corresponding author. E-mail: xmwswws@163.com

where φ denotes the flux in the nonlinear inductance L_2 and $n = 11$.

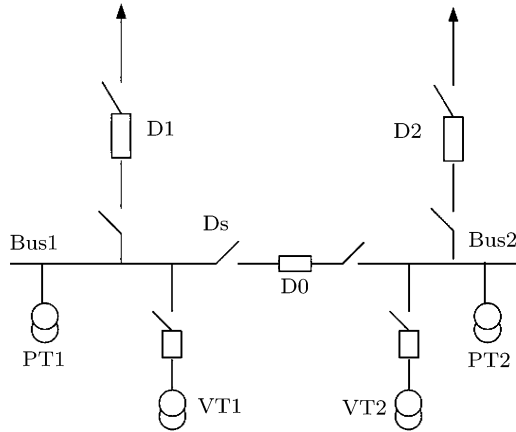


Fig.1. Typical ferroresonance circuit.

The core loss nonlinearity is modelled in the same way as described in Ref.[13]. A third-order polynomial given below is adequate for matching the nonlinear

characteristics:

$$i_{R_2} = h_0 + h_1 V_{R_2} + h_2 V_{R_2}^2 + h_3 V_{R_2}^3, \quad (2)$$

where the parameters are $h_0 = -3.5213 \times 10^{-3}$, $h_1 = 5.7869 \times 10^{-7}$, $h_2 = -1.4167 \times 10^{-12}$, and $h_3 = 1.21105 \times 10^{-18}$.

The differential equations for this circuit are

$$V_{R_2} = \frac{d\varphi}{dt}, \quad (3)$$

$$i = a\varphi + b\varphi^n + h_0 + h_1 V_{R_2} + h_2 V_{R_2}^2 + h_3 V_{R_2}^3, \quad (4)$$

$$E_m \sin(\omega t) = u_c + R_1 i + L_1 \frac{di}{dt} + V_{R_2}, \quad (5)$$

$$C \frac{du_c}{dt} = i. \quad (6)$$

In the nonlinear ordinary differential equations (3)–(6), φ , $\frac{d\varphi}{dt}$ and u_c are taken as state variables that are given as $x = \varphi$, $y = \frac{d\varphi}{dt}$, and $z = u_c$. Substituting these state variables into Eqs.(3)–(6) yields

$$\frac{dx}{dt} = y, \quad (7)$$

$$\frac{dy}{dt} = \frac{E_m \sin(\omega t) - z - y - R_1 (ax + bx^n + h_0 + h_1 y + h_2 y^2 + h_3 y^3) - L_1 (ay + nbx^{n-1}y)}{L_1 (h_1 + 2h_2 y + 3h_3 y^2)}, \quad (8)$$

$$\frac{dz}{dt} = \frac{ax + bx^n + h_0 + h_1 y + h_2 y^2 + h_3 y^3}{C}, \quad (9)$$

where ϕ is flux in inductance L_2 in p.u. value (per unit quantity), ω is the power frequency of 1.0 p.u. value.

3. Simulation results and discussion

In the following analysis, the effects of nonlinear core loss and linear core loss on the ferroresonance in a power system are presented. Equations (10)–(12) are the differential equations derived by using the linear

core loss model and state variables that are the same as those in Eqs.(7)–(9). To start with, the effect of varying the magnitude of the source voltage on the chaotic behaviour of the system is investigated. Bifurcation diagrams and phase-plane diagrams are two main tools to distinguish various modes of behaviour. Furthermore, the Lyapunov exponent is also used to distinguish chaotic states from steady states. For solving the differential equation system, the Matlab environment and an embedded package of fourth-order Runge–Kutta method are used by taking

$$\frac{dx}{dt} = y, \quad (10)$$

$$\frac{dy}{dt} = \frac{R_2 \left(E_m \sin(\omega t) - z - y - R_1 \left(ax + bx^n + \frac{y}{R_2} \right) - L_1 (ay + nbx^{n-1}y) \right)}{L_1}, \quad (11)$$

$$\frac{dz}{dt} = \frac{ax + bx^n + \frac{y}{R_2}}{C} \tag{12}$$

The initial conditions taken for simulation are $\omega = 1$, $E_m = 1$, $x = 0$, $y = 1.6$, and $z = 1.1$ in p.u value. The varying parameter is the magnitude of the source voltage E_m . In addition, the core loss R_2 is first taken as a nonlinear core loss and then compared with a linear resistance. Several cases and combinations are investigated, however, only the representative ones are presented here.

To classify the effects of varying source voltage E_m in Eqs.(7)–(9) on the behaviour of the system shown in Fig.2, extensive simulations are carried out. In order to predict which kind of ferroresonance may occur for a wide range of magnitude of source voltage change, the bifurcation diagram is obtained by changing R_2 between linear and nonlinear. Figure 3 shows the bifurcation diagrams for considering R_2 nonlinearity mentioned in Eq.(2); Figure 4 shows the bifurcation diagrams for considering R_2 as a linear model. The x -axis represents the magnitude of source voltage while the y -axis indicates the voltage across both ends of core loss R_2 .

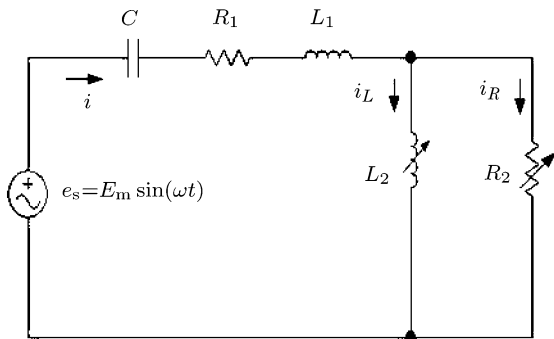


Fig.2. Thevenin equivalent circuit of Fig.1.

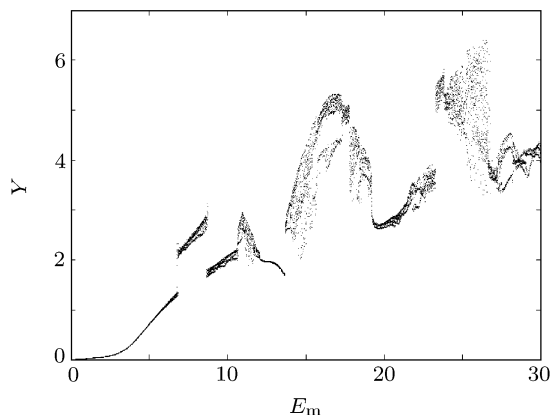


Fig.3. Bifurcation diagram for $n = 11$ and nonlinear model of core loss.

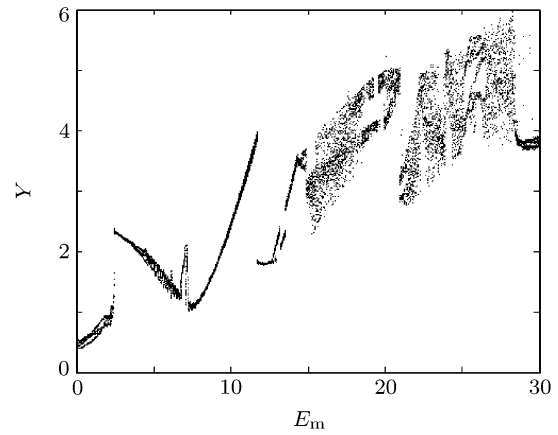


Fig.4. Bifurcation diagram for $n = 11$ and linear model of core loss.

The bifurcation diagrams shown in Figs.3 and 4 reveal what modes of ferroresonance are possible for a given excitation level. A single-value area of the bifurcation map indicates one period; a dual-value area indicates two periods, etc. In fact, subharmonics plays an important role in non-chaotic vibrations. One characteristic precursor to chaotic motion is the appearance of sub-harmonics. There exists a transitional region from periodic to chaotic, in which the waveform of V_{R_2} is still periodic but not sinusoidal as the source voltage and the trajectory in phase-plane change from limit cycle to strange attractors. Likewise, the region with many scattered points, which looks blurred as shown in Figs.3 and 4, indicates chaotic ferroresonance.

It can be observed from these figures that the bifurcation diagram with the nonlinear model of core loss has a shorter transient duration at a low excitation level, viz E_m less than 15 p.u. Furthermore, the magnitude of V_{R_2} overvoltage is limited to less than 3 p.u, with the nonlinear core loss model used. However, with using the linear core loss model the magnitude of V_{R_2} overvoltage can reach 4 p.u when E_m is near 12 p.u. Figure 5 shows the time domain wave form of V_{R_2} and phase plane diagram, with the linear core loss model used. Likewise, Fig.6 shows the time domain wave form of V_{R_2} and phase plane diagram with using the nonlinear core loss model. These figures reveal that, with the nonlinear core loss model used, the waveform of V_{R_2} becomes periodic after a short transient process while the maximum voltage of V_{R_2} becomes smaller. But with the linear core loss model used, the system is also in an unstable state. Furthermore, the orbit in phase plane changes from strange attractors to period limit cycles in the same way.

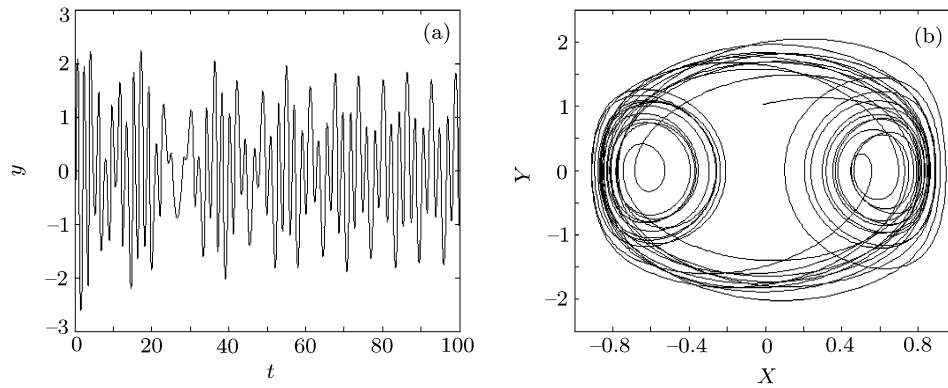


Fig.5. (a) Waveform and (b) phase plane orbit of $E_m = 5$, with the linear core loss model used.

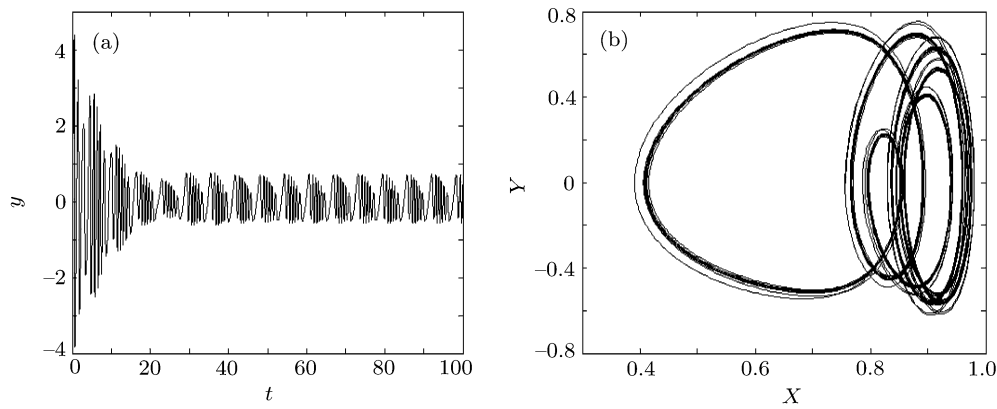


Fig.6. (a) Waveform and (b) phase plane orbit of $E_m = 5$ with the nonlinear core loss model adopted.

Moreover, Fig.7 shows the V_{R_2} waveform and phase plane diagram for $E_m = 20$, with the nonlinear core loss model used. Likewise, the V_{R_2} waveform and phase plane diagram for $E_m = 20$, with the linear core loss model used, are shown in Fig.8. The waveform of V_{R_2} (Fig.7(a)) is also periodic but not sinusoidal despite its starting with a non-periodic oscillation. The maximum magnitude of overvoltage is less than 2 p.u. Figure 7(b) indicates that the trajectory projected on the $X - Y$ plane is a limit cycle eventually. In addition, the Lyapunov exponents are calculated to be $\sigma_1 = -0.1673$, $\sigma_2 = -0.4813$, and $\sigma_3 = -235.4484$. There is no positive Lyapunov exponent, so the circuit is stable.

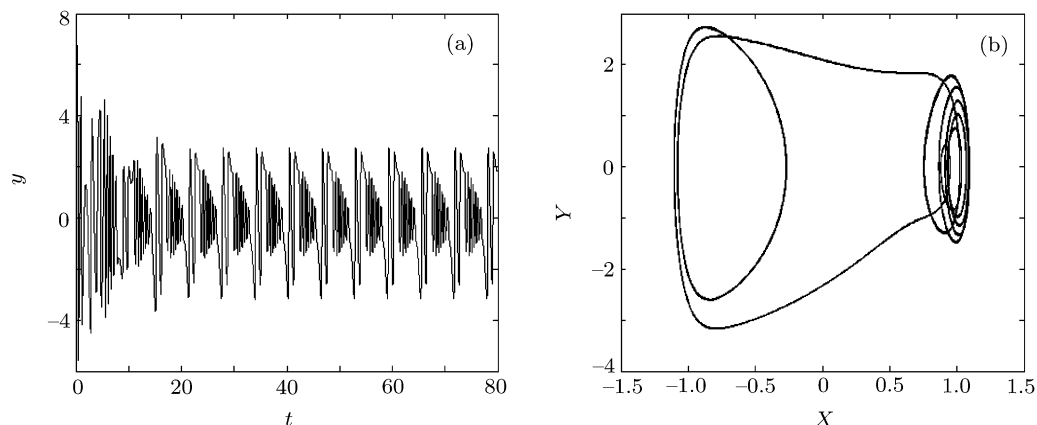


Fig.7. (a) Waveform and (b) phase plane orbit of $E_m = 20$, with the nonlinear core loss model used.

Unlike Fig.7, in Fig.8 the V_{R_2} waveform is distorted seriously compared with the sinusoidal waveform of source voltage. The maximum magnitude of overvoltage is more than 5 p.u. It is a very high voltage that can damage the distribution equipment. The Lyapunov exponents are calculated to be $\sigma_1 = 0.0552$, $\sigma_2 = -0.6549$, and $\sigma_3 = -302.9773$. The Lyapunov exponent is positive, so Fig.8(b) indicates that the trajectory has changed from limit cycles to strange attractors. It can be concluded from this simulation that with the nonlinear core loss model used, the onset of chaotic ferroresonance is at a larger excitation level than with the linear core loss model adopted.

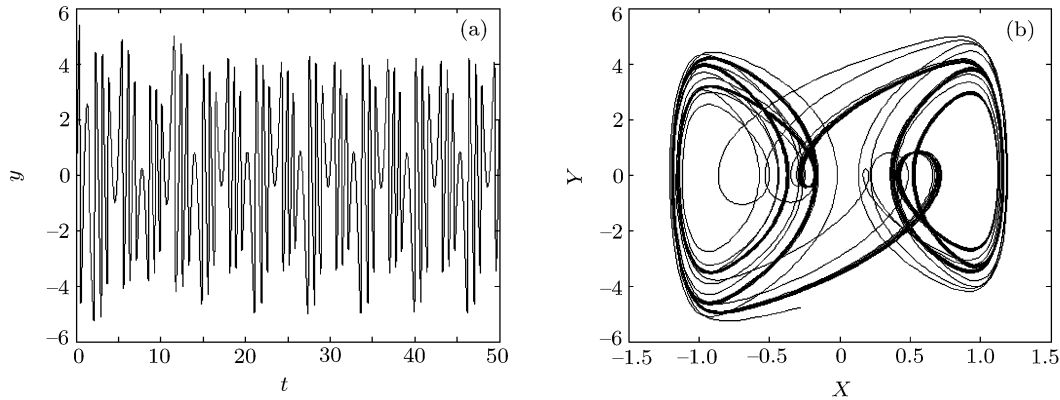


Fig.8. (a) Waveform and (b) phase plane orbit of $E_m = 20$ with the linear core loss model adopted.

4. Conclusions

Some results about the effects of nonlinear core loss on the behaviour of a typical ferroresonant circuit in a power system are obtained. The main conclusions drawn from the present study are (1) the inclusion of a nonlinear core loss model reveals that the solution of the system is optimistic compared with that with

the inclusion of a linear core loss model, (2) with using the nonlinear model of core loss the transient region is shorter than that using the linear core loss model, (3) the onset of chaotic ferroresonance is at a large source voltage. Since the ferroresonance modes become more accurate, ferroresonance could be prevented or mitigated.

References

- [1] Shen Y H and Zhi X 2008 *QingHai Electric Power* **27** 48 (in Chinese)
- [2] David A and Jacobson N 2003 *Power Engineering Society General Meeting* **2** 1206
- [3] Feng Y L and Shen K 2008 *Chin. Phys. B* **17** 0111
- [4] Edoardo B, Oriano B, Mario C, Gabriella C and Domenico G 2007 *J. Magnetism and Magnetic Materials* **316** 299
- [5] Hui M, Zhang Y B and Liu C X 2008 *Chin. Phys. B* **17** 3258
- [6] Si-Ma W X, Liu F, Sun C X, Liao R J and Yang Q 2006 *Acta Phys. Sin.* **55** 5714 (in Chinese)
- [7] Li Y G, Shi W and Li F R 2006 *IEEE Trans. Power Delivery* **21** 794
- [8] Liu F, Sun C X, Si-Ma W X, Liao R J and Guo F 2006 *Phys. Lett. A* **357** 218
- [9] Dick E P and Watson W 1981 *IEEE Trans. Power Apparatus and Systems* **100** 409
- [10] Marti J R and Soudack A C 1991 *IEE Proc-C* **138** 321
- [11] Al-Anbari K, Ramanujam R, Subba C.H R and Kuppusamy K 2002 *Electric Power Components and Systems* **30** 1015
- [12] Al-Anbari K, Ramanujam R, Subba C.H R and Kuppusamy K 2003 *Electric Power Systems Research* **65** 1
- [13] Washington L A and Hermann D 1993 *IEEE Trans. Power Systems* **8** 417